Steroids 75 (2010) 988–997

Contents lists available at ScienceDirect

Steroids

journal homepage: www.elsevier.com/locate/steroids

Effects of perinatal hypothyroidism on regulation of reelin and brain-derived neurotrophic factor gene expression in rat hippocampus: Role of DNA methylation and histone acetylation

Li Sui[a,*], Bao-Ming Li[b,c]

[a] Basic Medicine Laboratory, School of Medical Instrument and Food Engineering, University of Shanghai for Science and Technology, 516 Jun Gong Road, Shanghai 200093, China
[b] Institute of Neurobiology, Institutes of Brain Science, Fudan University, Shanghai 200032, China
[c] State Key Laboratory of Medical Neurobiology, Institutes of Brain Science, Fudan University, Shanghai 200032, China

ARTICLE INFO

Article history:
Received 11 May 2010
Received in revised form 10 June 2010
Accepted 10 June 2010
Available online 19 June 2010

Keywords:
Hypothyroidism
Epigenetic regulation
Reelin
BDNF
Hippocampus

ABSTRACT

Thyroid hormones have long been known to play important roles in the development and functions of the central nervous system, however, the precise molecular mechanisms that regulate thyroid hormone-responsive gene expression are not well understood. The present study investigated the role of DNA methylaion and histone acetylation in the effects of perinatal hypothyroidism on regulation of reelin and brain-derived neurotrophic factor (BDNF) gene expression in rat hippocampus. The findings indicated that the activities of DNA methyltransferase (DNMT), methylated reelin and BDNF genes were up-regulated, whereas, the activities of histone acetylases (HAT), the levels of global acetylated histone 3 (H3) and global acetylated histone 4 (H4), and acetylated H3, acetylated H4 at reelin promoter and at BDNF gene promoter for exon II were down-regulated in the hippocampus at the developmental stage of the hypothyroid animals. These results suggest that epigenetic modification of chromatin might underlie the mechanisms of hypothyroidism-induced down-regulation of reelin and BDNF gene expression in developmental rat hippocampus.

1. Introduction

Thyroid hormones (triiodothyronine, T3 and thyroxine, T4) exert well-defined effects on the development and function of the central nervous system. Thyroid hormone insufficiency during critical period of brain development results in permanent and profound effects on neurological functions that contribute to severe cognitive and neurological impairments [1,2]. T3, the active form of thyroid hormones, has been shown to act on the central nervous system via genomic (nuclear) and non-genomic pathways [3,4]. Thyroid hormone exerts its genomic actions by binding to its nuclear thyroid hormone receptors (TRs), which in turn bind to thyroid hormone response elements in the promoter region of thyroid hormone-responsive genes. In the presence of T3, TRs activate transcription by recruiting coactivator complexes, and in the absence of T3, TRs repress transcription by recruiting corepressor complexes [5].

A number of brain genes have been identified as regulated by thyroid hormones [6,7]. Among them, two genes, *reelin* and *brain-derived neurotrophic factor* (*BDNF*), which both play important roles in cell migration and neural plasticity during neural development and maintenance [8,9], have been shown to be responsive to thyroid hormone treatment [10–16]. However, the exact mechanism of thyroid hormone action on *reelin* or *BDNF* expression, whether transcriptional or post-transcriptional, remains to be determined.

DNA methylation, a covalent chemical modification of DNA, is catalyzed by DNA (cytosine-5) methyltransferases (DNMTs) and serves to repress gene transcription [17]. Histone acetylation, regulated by specific enzymes, including histone acetylases (HATs) and histone deacetylases (HDACs), relaxes chromatin structure, making it more accessible to transcriptional machinery. Thus, histone acetylation is associated with transcriptional activation [18]. Limited evidence has demonstrated that DNA methylation and demethylation [19,20] and histone acetylation and deacetylation [21–23] may play a role in regulating the transcriptional activity of T3-responsive genes. To expand our understanding of the molecular mechanisms of thyroid hormone action in the central nervous system, the effects of thyroid hormone insufficiency during development on DNA methylation and histone acetylation of *reelin* and *BDNF* at the level of gene transcription in rat hippocampus were investigated.

* Corresponding author. Tel.: +86 21 55271206; fax: +86 21 55270695.
E-mail addresses: lsui@usst.edu.cn, lsui@fudan.edu.cn (L. Sui).

0039-128X/$ – see front matter © 2010 Elsevier Inc. All rights reserved.
doi:10.1016/j.steroids.2010.06.005

2. Experimental

2.1. Animals and treatment

All animal procedures were carried out in accordance with the *NIH Guide for the Care and Use of Laboratory Animals*. Timed-pregnant Sprague–Dawley rats were obtained from the Shanghai Laboratory Animal Center, Chinese Academy of Sciences, China. These animals were housed individually and maintained on a 12 h light–dark cycle and in a temperature-controlled ($24 \pm 1\,^{\circ}C$) environment with access to food and water *ad libitum*. Some newborn rats were rendered hypothyroid by administering 0.05% (w/v) propylthiouracil (PTU) in the drinking water to their mothers from the 15th day of conception. Some hypothyroid pups received daily injections of T4 (0.02 μg/g body weight) dissolved in saline from day 1 after birth (postnatal day 1, PND 1) until death. It has been previously shown that this T4-injected rat is comparable to the euthyroid rat regarding the changes in body weight and plasma thyroid stimulating hormone (TSH) concentration [24–26]. The pup rats were sacrificed by decapitation on PND 1, 5, 15, 30 and PND 60, and the whole hippocampus, including subiculum, was dissected out. Tissues were frozen by liquid nitrogen and stored at $-80\,^{\circ}C$ until use.

2.2. Reagents

Primary antibodies: reelin (catalog no. sc-25346) and BDNF (catalog no. sc-546) were purchased from Santa Cruz Biotechnology, Inc. (Santa Cruz, CA, USA). Acetylated H3 (catalog no. 9671) and acetylated H4 (catalog no. 2594) were purchased from Cell Signaling Technology, Inc. (Beverly, MA, USA). EpiQuik™ nuclear extraction kit (catalog no. OP-0002-1), EpiQuik™ DNA Methyltransferase Activity/Inhibition Assay Kit (catalog no. P-3001), EpiQuik™ HAT Activity/Inhibition Assay Kit (catalog no. P-4003), EpiQuik™ Global Histone H3 Acetylation Assay Kit (catalog no. P-4008), EpiQuik™ Global Histone H4 Acetylation Assay Kit (catalog no. P-4009) and EpiQuik™ Tissue Chromatin Immunoprecipitation (ChIP) Kit (catalog no. P-2003) were purchased from Epigentek Group Inc. (Brooklyn, NY, USA). CpGenome™ Fast DNA Modification Kit (catalog no. s7824) was purchased from Chemicon International Inc. (Temecula, CA, USA). TIANamp Genomic DNA Kit (catalog no. DP 304) and TIANquick Midi Purification Kit (catalog no. DP 204) were obtained from TianGen Biotech Co. Ltd (Beijing, China). Trizol reagent (catalog no. 15596) was purchased from Invitrogen Corporation (Carlsbad, CA, USA). Real-time PCR Master Mix (SYBR Green) (catalog no. QPK-201) and RNA-direct Real-time PCR Master Mix (SYBR) (catalog no. QRT-201) was purchased from TOYOBO Co. Ltd (Osaka, Japan). The horseradish peroxidase (HRP)-conjugated goat anti-rabbit or mouse IgG, enhanced chemiluminescence (ECL) Western blotting detection reagents were obtained from Pierce Biotechnology (Rockford, IL, USA). Protease inhibitor cocktail and polyvinylidene difluoride (PVDF) membrane were obtained from Roche Products (Hertfordshire, UK). PTU, T4 and all other reagents were of analytical grade and from Sigma Chemical (St. Louis, MO, USA). Primers were synthesized by 391 DNA Synthesizer (PE Corporation, Norwalk, CT, USA).

2.3. Nuclear extracts and DNA methyltransferase activity assay

Nuclear extracts of the collected rat hippocampus were extracted (EpiQuik™ nuclear extraction kit, Epigentek Group Inc.), and then processed for DNMT activity measurement (EpiQuik™ DNA Methyltransferase Activity/Inhibition Assay Kit, Epigentek Group Inc.) by Tecan Infinite 200 microplate reader (Tecan Group Ltd., Männedorf, Switzerland). DNMT activity was expressed as optical density (OD) and the formula of DNMT activity (OD/h/ml) = (No inhibitor OD − blank OD)/sample volume added in the reaction × 1000 × sample dilution (if any), and Inhibition = 1 − OD (inhibitor sample − blank)/OD (no inhibitor control − blank).

2.4. DNA methylation assay

DNA was isolated from the rat hippocampus (TIANamp Genomic DNA Kit, TianGen Biotech Co. Ltd.) and purified (TIANquick Midi Purification Kit, TianGen Biotech Co. Ltd.) and processed for bisulfite modification (CpGenome DNA modification kit; Chemicon International Inc.). Quantitative real-time PCR was used to determine the DNA methylation status of the *reelin* and *BDNF* promoter according to the previously published study [27–29]. Because the structure of *BDNF* gene consists of nine promoters, which were mapping upstream of the nine 5′-exons (eight 5′ non-coding exons, exon I, II, III, IV, V, VI, VII, VIII, and a common exon IX encoding a preproBDNF mRNA) [30], however, exon II mRNA is the most abundant and can be detected during the developmental stage [13], thus, only *BDNF* promoter for exon II was investigated in the present study. For detection of unmethylated *reelin* DNA, the following primers were used: forward (5′-TGTTAAATTTTTGTAGTATTGGGGATGT-3′) and reverse (5′-TCCTTAAAATAATCCAACAACACACC-3′). Detection of methylated *reelin* DNA was performed using the following primer: forward (5′-GGTGTTAAATTTTTGTAGTATTGGGGAC-3′) and reverse (5′-TCCTTAAAATAAT CCAACAACACGC-3′). Detection of unmethylated *BDNF* DNA was performed using the following primers: forward (5′-GGGTAGTGATTTTGGGGAGGAAGTAT-3′) and reverse (5′-CAACCTCTATACACAACTAAATCCACC-3′). Primer sequences to detect methylated DNA in the *BDNF* promoter for exon II were as follows: forward (5′-GTAGCGATTTTGGGGAGGAAGTAC-3′) and reverse (5′-CAACCTCTATACGCGACTAAATCCG-3′). *Glyceraldehyde-3-phosphate dehydrogenase* (*GAPDH*) primers were used as controls: forward, 5′-AGGTCGGTGTGAACGGATTTG-3′; and reverse, 5′-TGTAGACCATGTAGTTGAGGTCA-3′. Each sample was run in triplicate in the presence of SYBR Green (Real-time PCR Master Mix). Reactions were run on an Mastercycler ep realplex real-time PCR machine (Eppendorf AG, Hamburg, Germany) with the following cycling program: 95 °C for 12 min, 40 cycles of 95 °C for 15 s, 60 °C for 15 min, and 72 °C for 45 s. Ct values from each sample were obtained using the Realplex software (Eppendorf AG, Hamburg, Germany). Relative quantification of template was performed as described previously [31,32] and by the Eppendorf manual. Detection of fluorescent products was at the end of the last step. For each sample, a ΔCt value was determined ($Ct_{reelin\ or\ BDNF} - Ct_{GAPDH}$), followed by a ΔΔCt value relative to the controls ($\Delta Ct_{hypothyroid\ group\ or\ hypothyroid+T4\ group} - \Delta Ct_{control\ group}$). Fold changes were determined by taking 2 to the power of ΔΔCt values. To further verify specificity of the final product, a melting curve analysis was carried out by the Mastercycler ep realplex (Eppendorf AG) and a single, well-defined peak in melting curve analysis demonstrates that only one amplification product is being produced.

2.5. Histone acetylation assay

2.5.1. Nuclear extracts and histone acetylases assay

Nuclear extracts of the rat hippocampus were extracted (EpiQuik™ nuclear extraction kit, Epigentek Group Inc.), and processed for the measurement of histone acetylases (EpiQuik™ HAT Activity/Inhibition Assay Kit, Epigentek Group Inc.) using the formula of HAT activity (OD/h/mg protein) = OD (untreated sample − blank)/h × protein amount (μg) added into the assay × 1000 and Inhibition % = 1 − OD (inhibitor sample − blank)/OD (no inhibitor control − blank) by Tecan Infinite 200 microplate reader (Tecan Group Ltd.).

2.5.2. Acid extracted histone and acetylation of histone H3/H4 assay

Total histones were extracted from the rat hippocampus with H_2SO_4, precipitated with trichloroacetic acid (TCA) and washed in 0.1%HCl/acetone and 100% acetone. The acetylation of histone H3 and histone H4 was measured by kits (EpiQuik™ Global Histone H3/H4 Acetylation Assay Kit, Epigentek Group Inc.) using the formula of Acetylation = OD (treated sample – blank)/OD (untreated control – blank) by Tecan Infinite 200 microplate reader (Tecan Group Ltd.).

2.5.3. Chromatin immunoprecipitation

The hippocampus was dissected and the tissue was finely chopped and incubated in freshly prepared 4% paraformaldehyde in phosphate buffered saline (PBS) for 20 min with gentle rocking. Crosslinking was halted by addition of 2.5 M glycine and an additional 5 min of gentle rocking. Samples were washed three times in PBS plus protease inhibitors (Roche Products), frozen by liquid nitrogen, and stored at −80 °C. The chromatin was solubilized and extracted by detergent lysis, followed by sonication. First, minced, fixed hippocampal tissue was homogenized in a homogenizing buffer (10 mM Tris, 10 mM NaCl, and 0.2% NP-40). The homogenate was centrifuged at 5500 × *g* for 5 min. The supernatant was decanted, and the pellet was homogenized using lysis buffer (50 mM HEPES–KOH pH 7.5, 140 mM NaCl, 1 mM EDTA pH 8.0, 1% Triton X-100, 0.1% sodium deoxycholate, 0.1% SDS, proteinase inhibitors). Next, the extracted chromatin was sheared to 400–800 bp using the Sonic Dismembrator 550 (Fisher Scientific, Hampton, NH, USA). Each sample was sonicated five times on ice, 20 s each, at 25% of maximum power. Chromatin immunoprecipitation (ChIP) assays were performed and the protocol outlined in the EpiQuik™ Tissue ChIP kit (Epigentek Group Inc.) was used. After the chromatin lysate was extracted and properly fragmented to 400–800 bp, the chromatin lysate were diluted with ChIP dilution buffer at a 1:1 ratio. 10 μl of the pre-immunoprecipitated lysate was saved as "input" for later normalization. The chromatin solution was then immunoprecipitated 1.5 h at room temperature with 5 μg of primary antibody directed against acetylated H3 (Cell Signaling Technology, Inc.) and acetylated H4 (Cell Signaling Technology, Inc.) in the ChIP kit strip wells. As a control, samples were immunoprecipitated with 5 μg nonimmune rabbit IgG. After immunoprecipitation, the DNA–protein complex was then eluted and proteins were digested with DNA release buffer and proteinase K. DNA was dissociated at 65 °C for 1.5 h under reverse buffer. The DNA, associated with acetylated H3 or acetylated H4, was extracted with binding buffer, precipitated with 70% and 90% ethanol, and finally elute purified DNA by elution buffer. DNA was analyzed by spectrophotometer (Eppendorf AG, Hamburg, Germany) to confirm DNA quality. Quantitative real-time PCR was performed with primers specific to the *reelin* and *BDNF* gene promoters. Specific primers were designed to amplify proximal promoter regions. For *reelin*, the forward primer was 5′-AAAGGGAGATTGGGTGACG-3′ and the reverse primer was 5′-ACGTGCTTCTGGATGGTTTC-3′ [32]. For *BDNF* exon II, the forward primer was 5′-TGAGGATAGGGGTGGAGTTG-3′ and the reverse primer was 5′-GCAGCAGGAGGAAAAGGTTA-3′ [32]. *GAPDH*, the forward primer 5′-CCTGCCAAGTATGATGACATCAA-3′ and the reverse primer 5′-AGCCCAGGATGCCCTTTAGT-3′, was used as the internal standard. Input and immunoprecipitated DNA amplification reactions were run in triplicate in the presence of SYBR Green (Real-time PCR Master Mix). Relative quantification of template was performed as described previously. Each PCR reaction, run in triplicate for each brain sample, was repeated at least two independent times. All primer sets had comparable efficiency of amplification. After amplification, the specificity of the PCR products was verified by a melting curve analysis by the Mastercycler ep realplex (Eppendorf AG).

2.6. Measuring mRNA levels by real-time RT-PCR

The whole hippocampus of control rats, hypothyroid rats and hypothyroid + T4 injection rats was collected for RNA quantification. RNA was extracted using Trizol reagent (Invitrogen Corporation), precipitated with isopropanol and purified by DNase treatment. Relative quantification of *reelin* and *BDNF* exon II mRNA levels was done using real-time RT-PCR (Mastercycler ep realplex). The following primers were used to amplify specific regions of the transcripts of interest: *reelin* (5′-AAACTACAGCGGGTGGAACC-3′ and 5′-ATTTGAGGCATGACGGACCTATAT-3′), *BDNF* exon II (5′-CCATAAGGACGCGGACTTGTAC-3′ and 5′-AGACATGTTTGCGGCATCCAGG-3′) and *GAPDH* (5′-AACGACCCCTTCATTGAC-3′ and 5′-TCCACGACATACTCAGCAC-3′). *GAPDH* quantification was used as an internal control. One-step RT-PCR was performed using RNA-direct SYBR Green Real-time PCR Master Mix Kit (TOYOBO Co.). Total reaction volume was 50 μl containing 2 μg total RNA and 0.2 μM of each primer. $Mn(OAc)_2$ concentration was 50 mM. Reaction conditions were chosen according to the manufacturer's recommendations. Reverse transcription was performed at 61 °C for 20 min followed by denaturation at 95 °C for 60 s. PCR cycles consisted of three steps: denaturation at 95 °C for 15 s, annealing at 55 °C for 15 s and elongation at 74 °C for 45 s. In total, 45 cycles were performed. Fluorescence was measured at the end of each elongation step at 74 °C. After amplification, the specificity of the PCR products was also verified by a melting curve analysis. Fold differences of mRNA levels over the control values were calculated using the $\Delta\Delta$Ct method as described above. PCR reactions were run in triplicate for each brain sample, and repeated at least two independent times.

2.7. Western blotting

The method for Western blotting has been described previously [33,34]. Briefly, hippocampal tissues were homogenized with ice-cold lysis buffer (1% Triton X-100, 5 mM EDTA, 10 mM Tris, 1% SDS, 1% NP-40, 10 mM deoxychdate, 60 mM CHAPS, 1 mM NaF, 1 mM Na_3VO_4, 1 mM PMSF and complete protease inhibitor cocktail) for 30 min. Samples were sonicated and spun down at 15,000 × *g* at 4 °C for 10 min. Protein concentrations were determined by a BCA protein assay. The supernatant protein samples were boiled at 100 °C for 3 min in loading buffer (10% SDS, 1 M Tris–HCl, 20% glycerol, 0.2 M dithiothreitol, and 0.02% bromphenol blue). Equal protein extracts were then separated by denaturing SDS-polyacrylamide gels on a 10% resolving gel with a 4% stacking gel and transferred onto a PVDF membrane. The PVDF membranes were blocked in 5% non-fat dry milk for 2 h at room temperature in Tris-buffered saline (0.1% Tween 20, 50 mM Tris–HCl pH 7.5, 150 mM NaCl) containing Tween 20 (TBST). The membranes were then hybridized overnight with primary antibodies in primary buffer (5% non-fat dry milk in TBST). This was followed by three washes in TBST and incubation for 2 h with a secondary HRP-conjugated goat antibody diluted 1:2000 in primary buffer. The membranes were washed in TBST and blots were developed using ECL and exposed to X-ray film. The dilution of the antibodies of reelin and BDNF was 1:500. Densitometric analysis of immunoreactivity for proteins was conducted using a Bio-Rad Image Analysis System. Western blot data were compiled from at least four independent animals at each time point.

2.8. Thyroid hormone level testing

Rats' trunk blood at the time they were sacrificed was collected to clot on ice for a minimum of 30 min. Serum was separated via centrifugation of clotted samples and stored at −80 °C for later

Table 1
Mean serum total T3 and total T4 levels in the testing animals.

	Control	PTU-exposed	T4-injected hypothyroid
Total T3 (nmol/l)			
PND 1	0.62 ± 0.16 (n = 10)	Below the sensitivity[a,#]	0.45 ± 0.18 (n = 7)
PND 5	1.02 ± 0.18 (n = 8)	Below the sensitivity[a,#]	0.82 ± 0.19 (n = 7)
PND 15	1.98 ± 0.12 (n = 8)	0.47 ± 0.17 (n = 8)[#]	1.71 ± 0.18 (n = 7)
PND 30	1.84 ± 0.15 (n = 7)	0.62 ± 0.19 (n = 8)[#]	1.67 ± 0.20 (n = 6)
PND 60	1.36 ± 0.13 (n = 8)	1.12 ± 0.17 (n = 8)	1.18 ± 0.21 (n = 6)
Total T4 (nmol/l)			
PND 1	32.22 ± 8.52 (n = 10)	Below the sensitivity[a,#]	20.53 ± 9.82(n = 7)
PND 5	51.44 ± 8.13 (n = 8)	Below the sensitivity[a,#]	45.79 ± 7.88 (n = 7)
PND 15	90.92 ± 8.32 (n = 8)	Below the sensitivity[a,#]	95.92 ± 8.32 (n = 7)
PND 30	64.58 ± 7.96 (n = 7)	20.72 ± 8.84 (n = 8)[#]	67.82 ± 9.18 (n = 6)
PND 60	60.72 ± 8.53 (n = 8)	50.42 ± 9.03 (n = 8)	66.75 ± 7.35 (n = 6)

[a] A large portion of samples (>80%) of pups at PND 1–15 from the PTU-exposed group had total T3 and total T4 estimates which fell below the minimal detectable concentration of the T3 assay (0.18 nmol/l) and the T4 assay (1.28 nmol/l).
[#] Significantly different from the control group (P < 0.05). Values below the sensitivity in the PTU-exposed group were set to the minimal detectable concentration of the T3 assay (0.18 nmol/l) and the T4 assay (1.28 nmol/l) for statistical purposes. Samples from all other groups were above the minimal detectable concentration.

analyses by commercially available radioimmunoassay kit (Chemclin Biotech Co., Beijing, China). Serum concentrations of total T3 and total T4 were analyzed by radioimmunoassay. All samples for total T3 and total T4 were run in duplicate and the intra- and inter-assay variations were less than 10%. The sensitivity of the radioimmunoassay for total T3 and total T4 was 0.18 nmol/l and 1.28 nmol/l, respectively.

2.9. Statistical analysis

All values were taken as the mean ± SEM. For comparison between treatment groups, statistical analysis was performed by analysis of variance (ANOVA) using the general linear model procedure followed by separation of means using Least Significant Difference. The criterion for significance was set at P < 0.05.

3. Results

3.1. Developmental effects of PTU treatment on thyroid hormone levels

PTU induces hypothyroidism by inhibiting thyroid iodination and has been used as a typical thyroid antagonist [35]. Exposure of pregnant rat to 0.05% (w/v) PTU from day 15 post-conception until weaning significantly reduced circulating total T3 and total T4 levels in the pups at the developmental stage, but these reductions could be reversed by the injection of T4 in the hypothyroid animals. The data of the circulating total T3 and total T4 levels in the controls, the PTU-exposed, the T4-injected hypothyroid rats were presented in Table 1. In addition, the litter size, pup survival rate, and the number of dams that had successful deliveries were significantly lower in the 0.05% PTU treatment group (all P < 0.05, data not shown), which were comparable with the previous studies [24,25].

3.2. Hypothyroidism-induced up-regulation in DNA methylation

To determine whether methylation of *reelin* and *BDNF* genes in the developmental and adult rat hippocampus is altered by perinatal hypothyroidism, the activities of total DNMT, major enzymes involved in establishing genomic methylation patterns, were measured firstly by customized assay kits. The ratio or amount of methylated DNA, which is proportional to enzyme activity, can be colorimetrically quantified through an Enzyme-Linked ImmunoSorbent Assay (ELISA)-like reaction. As shown in Fig. 1A, the activities of DNMT in rat hippocampus in the controls increase with development and become maximal at PND 5 (~150% relative to PND 1, 100%), and then decline, exhibiting age-dependent manner. In the hypothyroid animals, the overall activities of DNMT in the hippocampus also displayed development-dependent, even though the maximal DNMT activities were found at PND 1 (Fig. 1A).

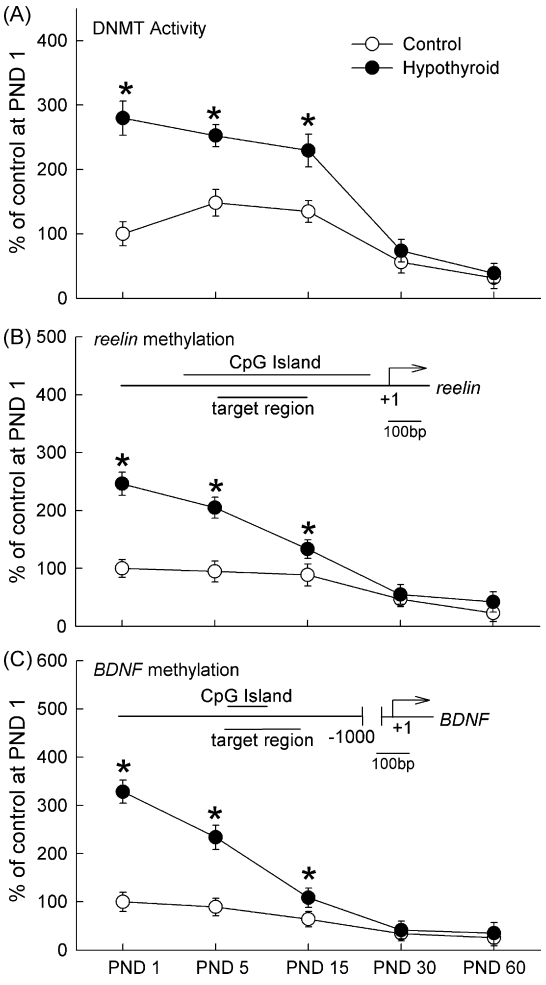

Fig. 1. Percent changes of DNMT activities (A), methylation of *reelin* (B) and methylation of *BDNF* (C) in rat hippocampus of the hypothyroid (n = 6 at each PND) and the controls (n = 6 at each PND) as a function of postnatal developmental and adult stage. Mean values of the controls at PND 1 were set as 100%. *P < 0.05 vs. the control group at the same age. Insets, schematic representation of the location of the CpG island in the *reelin* (B) and *BDNF* exon II (C) promoter regions relative to the transcription initiation site. Primer sets were designed to amplify the target regions. The scale bar represents 100 bp.

Comparison between the control and the hypothyroid groups, significant up-regulation in the activities of DNMT was found at PND 1, PND 5 and PND 15 in the hypothyroid groups ($F(1,10) \geq 6.37$, P's < 0.05), and no significant difference was found at PND 30 and PND 60 ($F(1,10) \leq 4.73$, both P's > 0.05).

Alterations in the activities of DNMT may contribute to the changes of methylation status of target genes, the levels of unmethylated and methylated *reelin* and *BDNF* were thus quantified, respectively, by quantitative real-time PCR using the specific primers. The ratios of levels of methylation to unmethylation for each gene were calculated. Development-dependent decline of methylated *reelin* (Fig. 1B) and methylated *BDNF* (Fig. 1C) in rat hippocampus was observed in the control and the hypothyroid groups. Compared with the controls, significant increases in the methylation of *reelin* (Fig. 1B) and *BDNF* (Fig. 1C) in the hippocampus were found at PND 1, PND 5 and PND 15 in the hypothyroid group ($F(1,10) \geq 5.55$, P's < 0.05). No significant increase was found at PND 30 and PND 60 in the hypothyroid group relative to the controls.

Likewise, the activities of DNMT, the methylation and the unmethylation status of *reelin* and *BDNF* genes in the developmental and young adult hippocampus were examined in the T4-injected hypothyroid rats (data not shown in the figures). No significant difference was found between the T4-injected hypothyroid and the control groups, indicating that the perinatal hypothyroid-induced increase in DNA methylation in rat hippocampus at the early developmental stage can be rescued by thyroid hormone restore.

3.3. Hypothyroidism-induced down-regulation in histone acetylation

To determine whether perinatal hypothyroidism-induced alterations in histone acetylation in the developmental and young adult rat hippocampus, the total activities of HAT and global acetylated H3, global acetylated H4 were determined in the hypothyroid and the control groups. As shown in Fig. 2A, the activities of HAT increased with postnatal development and became maximal at PND 15, and then decreased with age in the controls. Even though the pattern of age-dependent activities of HAT in the hippocampus was also mirrored in the hypothyroid animals, however, the activities of HAT were significantly decreased at each developmental stage except at PND 60 in the hypothyroid group relative to the controls ($F(1,10) \geq 6.53$, P's < 0.05) (Fig. 2A). The levels of global acetylated H3 and global acetylated H4 were also measured by customized assay kits in rat hippocampus. During the time course of development, the levels of global acetylated H3 (Fig. 2B) and global acetylated H4 (Fig. 2C) in the controls were stable and no age-dependence was observed. Compared with the controls, global acetylated H3 was significantly decreased at PND 1, 5, 15 and 30 ($F(1,10) \geq 5.42$, P's < 0.05), but not at PND 60 in the hypothyroid group (Fig. 2B). Similarly, but a slightly different from the global acetylated H3, the global acetylated H4 was significantly down-regulated at PND 1, 5 and 15, but not at PND 30 and PND 60, in the hypothyroid group (Fig. 2C).

Likewise, the HAT activities, the global acetylated H3 and H4 levels in the developmental and young adult hippocampus were also detected in the T4-injected hypothyroid rats. The analysis data did not reveal any significant differences between the T4-injected hypothyroid group and the controls (data not shown), indicating that the hypothyroid-induced down-regulation of total histone acetylation can be reversed by thyroid hormone supplement.

To better understand whether the associations of acetylated H3 and acetylated H4 at the *reelin* promoter and at *BDNF* gene promoter for exon II were affected by perinatal hypothyroidism, acetylated H3, acetylated H4 at the *reelin* promoter and at *BDNF* gene promoter for exon II in rat hippocampus were quantified in the control, the hypothyroid and the T4-injected hypothyroid groups, respectively, using ChIP assays with antibodies specific against acetylated H3 and acetylated H4. The amount of DNA associated with these acetylated antibodies was quantified using real-time PCR.

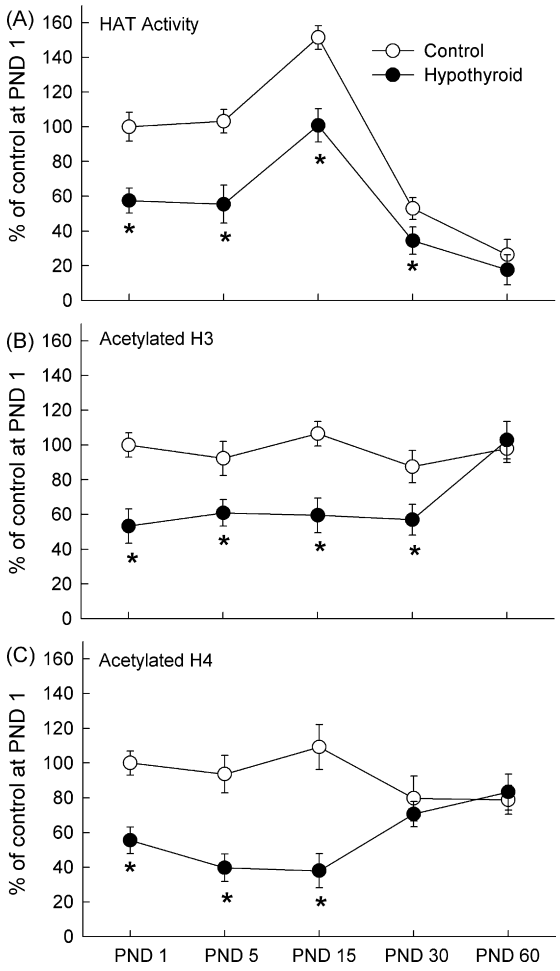

Fig. 2. Percent changes of HAT activities (A), global acetylated H3 (B) and global acetylated H4 (C) in rat hippocampus of the hypothyroid ($n = 5$ at each PND) and the controls ($n = 6$ at each PND) as a function of postnatal developmental and adult stage. Mean values of the controls at PND 1 were set as 100%. *$P < 0.05$ vs. the control group at the same age.

In ChIP assays, to confirm the specificity of antibody binding, hippocampal chromatin samples immunoprecipitated with nonimmune IgG were performed. The data revealed that nonimmune IgG precipitated negligible levels of the genes studied (Fig. 3A). In addition, association of acetylated H3 and acetylated H4 at the promoters of *glyceraldehyde-3-phosphate dehydrogenase* (*GAPDH*) was examined in the control, the hypothyroid and the T4-injected hypothyroid groups, and the association levels did not differ among the three treatment animals (Fig. 3A). To avoid bias caused by differences in PCR efficiency between the three group PCR reactions, a serial dilution of input material was acted as a standard curve for each PCR. A line representing the best fit is calculated for a standard curve using the least squares method of linear regression: $y = mx + b$ where $y = \text{Ct}$, $m = \text{slope}$, $x = \log_{10}$ template amount, and $b = y$-intercept (Fig. 3B). In the real-time PCR experiments, PCR product melting curve analysis at the end of the PCR confirmed a single product of the PCRs (Fig. 3C). These procedures confirm that the observed changes in the association of acetylated H3 and acetylated H4 to the *reelin* promoter and to the *BDNF* promoter for exon II, which are presented below, are specific to the treatment.

As shown in Fig. 4, the levels of association of acetylated H3, acetylated H4 at *reelin* promoter and at *BDNF* promoter for exon II were significantly decreased at a certain developmental stage in the hypothyroid rats relative to the controls. Specifically, the levels of acetylated H3 (Fig. 4A) and acetylated H4 (Fig. 4B) at the *reelin* promoter were significantly decreased at PND 1, PND 5 and PND 15, but not at PND 30 and PND 60 in the hypothyroid group. The levels of acetylated H3 at the *BDNF* promoter for exon II were significantly decreased at PND 1, 5, 15 and PND 30 in the hypothyroid animals (Fig. 4C). The levels of acetylated H4 at the *BDNF* promoter for exon II were significantly decreased at PND 1, 5 and PND 15, but not at PND 30 and PND 60 in the hypothyroid animals (Fig. 4D). In

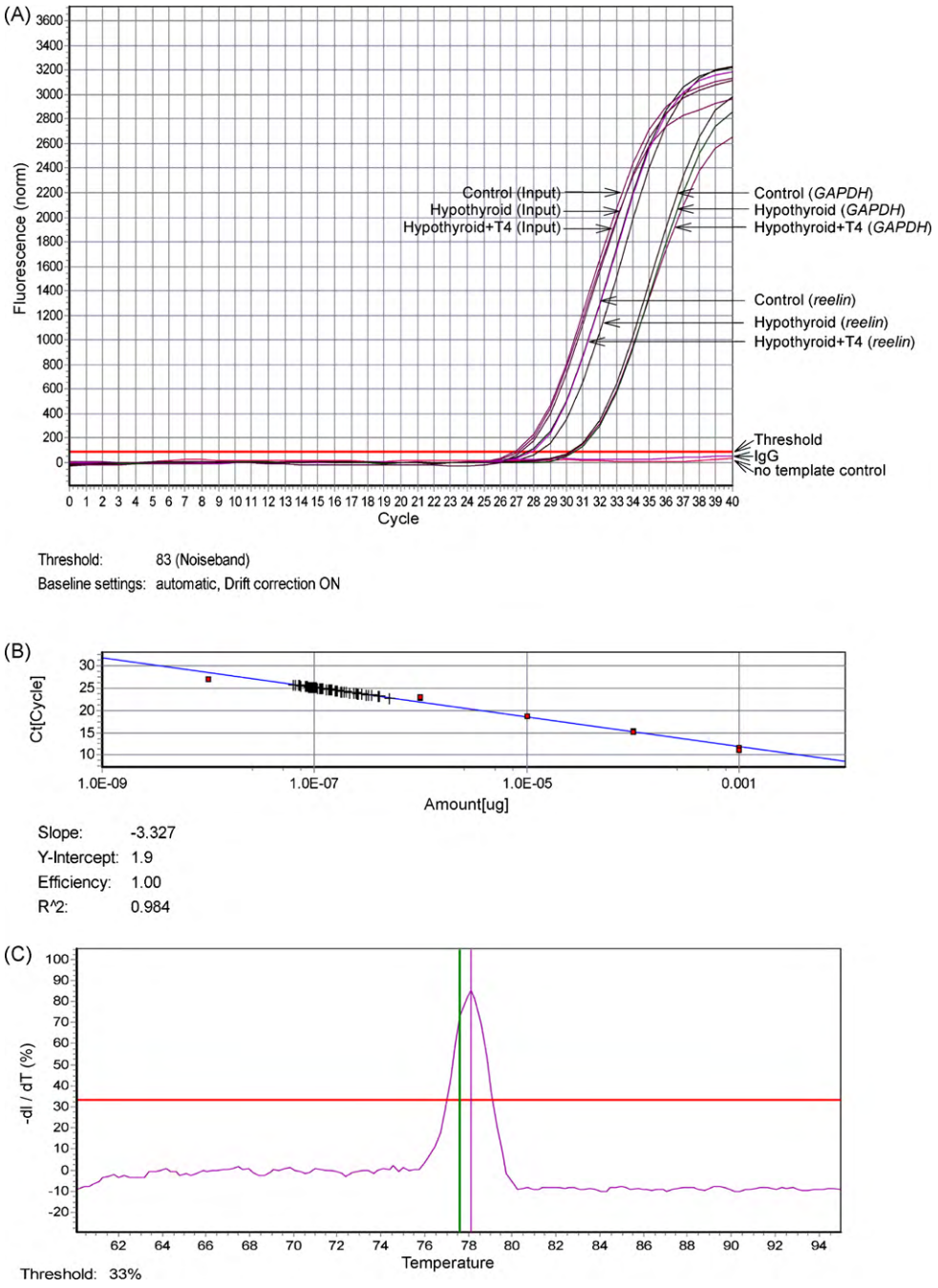

Fig. 3. (A) Representative quantification of acetylated H3 at *reelin* promoter in the hippocampus of the control, the hypothyroid and the hypothyroid restore rats was presented by real-time PCR Realplex software (Eppendorf AG, Hamburg, Germany). A threshold of 83 was automatically set by the software. Ct values of the control, the hypothyroid and the hypothyroid + T4 groups were normalized to the Ct values obtained from "Input" or non-immunoprecipitated genomic DNA, at which there is no difference among the control, the hypothyroid and the hypothyroid + T4 groups, as expected. Comparison of these Ct values revealed a significant decrease in levels of acetylated H3 at *reelin* promoter in the hypothyroid group vs. the control group, the hypothyroid + T4 group. In aliquots of the same samples, Ct values from the *GAPDH* gene differed by a negligible 0.1–0.3, reflecting no regulation by the hypothyroid or hypothyroid + T4 treatment. Immunoprecipitation with nonimmune IgG yielded no obvious Ct value, indicating a negligible precipitation of the *reelin* gene in the absence of specific antibody. Parallel experimental data for quantification of levels of acetylation H4 at *reelin* promoter or at *BDNF* promoter for exon II was not shown. (B) Representative standard curve was created by real-time PCR Realplex software (Eppendorf AG, Germany). The slope of the standard curve, y-intercept (an indication of the sensitivity of the assay and how accurately the template is quantified), efficiency (equal to $[10^{(-1/\text{slope})}] - 1$) and R^2 (coefficient of determination) were included. (C) An illustration of the use of melting curve analysis to distinguish specific PCR products. A single, well-defined peak in melting curve analysis demonstrates that only one amplification product is being produced.

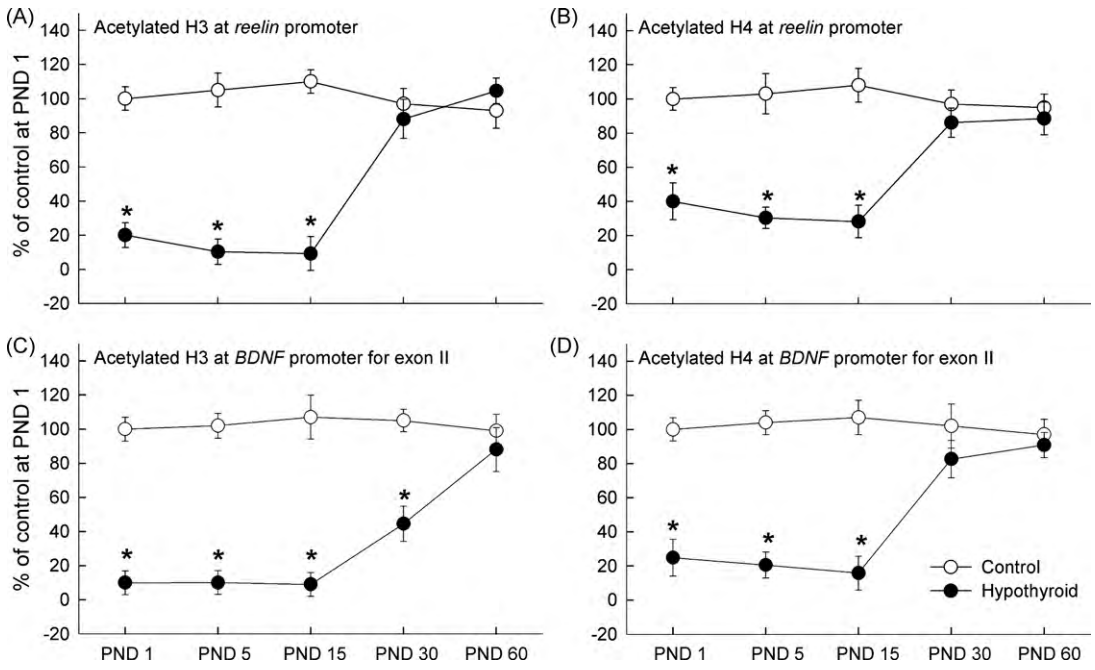

Fig. 4. Percent changes of recruitment levels of acetylated H3 (A) and acetylated H4 (B) to *reelin* promoter, and recruitment levels of acetylated H3 (C) and acetylated H4 (D) to *BDNF* promoter for exon II in rat hippocampus of the hypothyroid ($n = 5$ at each PND) and the controls ($n = 5$ at each PND) as a function of postnatal developmental and adult stage. Mean values of the controls at PND 1 were set as 100%. $^*P < 0.05$ vs. the control group at the same age.

addition, the association of acetylated H3 and acetylated H4 at the *reelin* promoter and at the *BDNF* promoter for exon II during the developmental period in the controls did not show any significant age-dependence. Likewise, the levels of association of acetylated H3, acetylated H4 at the *reelin* promoter and at the *BDNF* promoter for exon II in the T4-injection hypothyroid group were assayed. The analysis results did not find any significant differences between the T4-injected hypothyroid and the control groups (data not shown in figures), implying that the hypothyroid-induced decrease in the acetylated H3, acetylated H4 at the *reelin* and *BDNF* promoter for exon II could be completely reversed by thyroid hormone restore.

These results indicated that perinatal hypothyroidism reduced the activities of HAT, the global acetylated H3 and the global acetylated H4 levels, and the levels of association of acetylated H3 and acetylated H4 at the *reelin* promoter and at the *BDNF* promoter for exon II in rat hippocampus, especially at the developmental stage. In addition, these alterations were specific to the perinatal hypothyroidism and could be totally rescued by thyroid hormone supplement during development.

3.4. Hypothyroid-induced decreases in the reelin and BDNF exon II mRNA and protein expression

To test the degree to which DNA methylation and association of acetylated H3, acetylated H4 to the promoters of *reelin* and *BDNF* exon II correlates with the transcriptional activity of these genes, *reelin* and *BDNF* exon II mRNA levels in the hippocampus in the control, the hypothyroid and the T4-injection hypothyroid groups were quantified using real-time RT-PCR. As shown in Fig. 5, the *reelin* mRNA expression in the controls decreased (Fig. 5A), whereas, the *BDNF* exon II mRNA expression was increased with developmental stage (Fig. 5B). Furthermore, significant decreases in the *reelin* mRNA expression was observed at PND 1, PND 5 and PND 15 in the hypothyroid group relative to the controls ($F(1,8) \geq 6.77$, P's < 0.05, Fig. 5A). The *BDNF* exon II mRNA expression significantly decreased at PND 1, 5, 15 and PND 30 ($F(1,8) \geq 12.58$, P's < 0.01), but not at PND 60 in the hypothyroid animals (Fig. 5B).

Real-time RT-PCR method was also used to examine the *reelin* and *BDNF* exon II mRNA expression in the T4-injected hypothyroid group. No significant difference was found between the T4-injected hypothyroid and the control groups (data not shown), indicating that hypothyroidism-induced alterations in the *reelin* and *BDNF* exon II mRNA expression can be restored by thyroid hormone supplement.

Similarly, the protein content for *reelin* and *BDNF* in the hippocampus was determined in the control, the hypothyroid and the T4-injected hypothyroid animals as well. The patterns of reelin (Fig. 5C), BDNF protein (Fig. 5D) expression and the reduction of these two proteins in the hypothyroid groups were comparable to those of mRNA expressions. Furthermore, these significant decreases in the reelin and BDNF protein levels can be reversed by the thyroid hormone restore in the T4-injected hypothyroid group. These findings indicated that, for the *reelin* and *BDNF* genes, levels of protein expressions correlated with transcriptional levels and the abundance of mRNAs generally reflects the abundance at the protein levels.

4. Discussion

In the present study we have addressed the molecular mechanism by which perinatal hypothyroidism induced by administration of PTU into the dinking water of the dams from the fifteen day after conception and until weaning affects *reelin* and *BDNF* gene expression in the developmental and young adult hippocampus. Our findings demonstrated that perinatal hypothyroidism up-regulated the activities of DNMT, and methylated *reelin* and *BDNF* expression, whereas, down-regulated the activities of HAT, global acetylated H3 and global acetylated H4 levels, acetylated H3, acetylated H4 at *reelin* promoter and at *BDNF* gene promoter for exon II, as well as *reelin* and *BDNF* exon II mRNA and protein expression in the hippocampus at the early developmental stage. All these results raise the possibility that epigenetic modification of *reelin* and *BDNF* gene might be understood as a mechanism of devastative effects of perinatal hypothyroidism on the central nervous system.

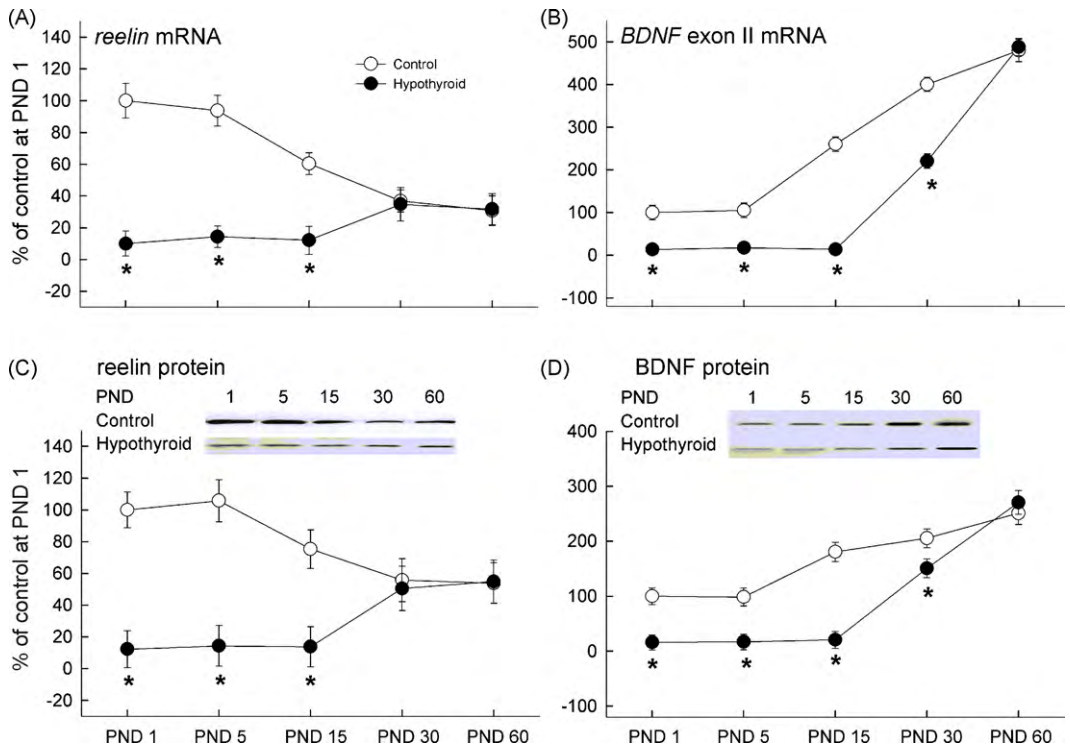

Fig. 5. Percent changes of *reelin* mRNA expression (A), *BDNF* exon II mRNA expression (B), reelin protein expression (C) and BDNF protein expression (D) in rat hippocampus of the hypothyroid ($n = 6$ at each PND) and the controls ($n = 6$ at each PND) as a function of postnatal developmental and adult stage. Insets are representative Western blots for PND 1–60 of the control and the hypothyroid groups. Reelin 420 kDa, BDNF 12.3 kDa. Mean values of the controls at PND 1 were set as 100%. $^*P < 0.05$ vs. the control group at the same age.

At the molecular level, epigenetic modification of chromatin involves chemical changes to the DNA and associated proteins [36–38]. DNA methylation and histone acetylation are major epigenetic modifications that play critical roles in gene expression reprogramming during development and differentiation. DNA methylation is an essential mechanism for the normal development of different organisms including mammals and plants, and has been implicated in the silencing of gene expression [36]. DNA methylation is carried out by two types of DNMTs: *de novo* (DNMT3A and DNMT3B) and maintenance methyltransferases, DNMT1 [39,40]. Disruption of any of these three major DNMTs is associated with global methylation status [41,42]. In the present study, the activities of total DNMTs in the hippocampus were up-regulated in the hypothyroid animals at the early developmental stage, which may result in the increase in the global DNA methylation in the hypothyroid hippocampus. We further demonstrated that the methylation of two genes, *reelin* and *BDNF*, was also up-regulated in the hypothyroid hippocampus at the same early developmental stage as that for the activities of DNMT. These results suggest that some thyroid hormone-responsive genes may undergo epigenetic modification of DNA methylation at the very early developmental stage. Supporting this suggestion, previous studies also demonstrated that the level of methylation of the rat hepatic S14 gene, a thyroid hormone-regulated gene, was increased in the hypothyroid animals [19,20]. Moreover, all these studies indicated that the level of methylation was reversible as the thyroid state was altered [19,20], consisted with our results.

It has been known that DNA methylation can directly recruit binding proteins that interfere with basal transcriptional machinery or can recruit histone deacetylases that further compact the chromatin and thus suppress gene transcription [43]. Perinatal hypothyroidism-induced increases in the methylation of *reelin* and *BDNF* genes could lead to suppressing expression of *reelin* and *BDNF*. In the present study, the time window of increased methylation of *reelin* gene was the same as that of reduced *reelin* mRNA and protein expression (all at PND 1, 5, and 15), however, the time window of the methylation of *BDNF* gene (PND 1, 5 and 15) and the alteration of *BDNF* exon II expression (PND 1, 5, 15 and 30) was not matched. These results suggest that epigenetic modulation of DNA methylation might partly contribute to the alterations of thyroid hormone-responsive gene expression, some other factors may influence the transcriptional activities.

Histone acetylation and deacetylation, another epigenetic modification, also regulate the gene expression and the role for histone acetylation and deacetylation in regulating the transcriptional activity of thyroid hormone-responsive genes has been demonstrated in various cell lines [44–46]. For example, in the cardiac myocyte, HAT has been shown to be involved in the thyroid hormone-activated gene transcription [21]. However, there is limited evidence that histone acetylation can regulate gene expression in the central nervous system. In this study, the activities of HAT in the hippocampus were reduced in the hypothyroid animals at the developmental stage (PND 1-PND 30), which is consistent with the previous findings of expression of HDACs (including HDAC1and HDAC2, enzymes that selectively deacetylate histone proteins) altered significantly in the cerebellum of the hypothyroid animals [47].

It is now known that thyroid hormone-induced activation of gene transcription is a two-step process: initially requires chromatin remodeling by HATs followed by the release of HATs and the recruitment of other coactivator proteins to promote transcription [46,48]. Some transcriptional coacticvators, such as steroid receptor coactivator-1 (SRC-1), cAMP response element-binding protein (CBP), and P300/CBP-associated factor (PCAF), have HAT activity [49]. In addition, sustained histone acetylation induced by trichostatin A (TSA), a HDAC inhibitor, could inhibit histone deacetylation and affect the T3-mediated gene transcription [21,50]. All these indicate a role of histone acetylation in the regulation of thyroid

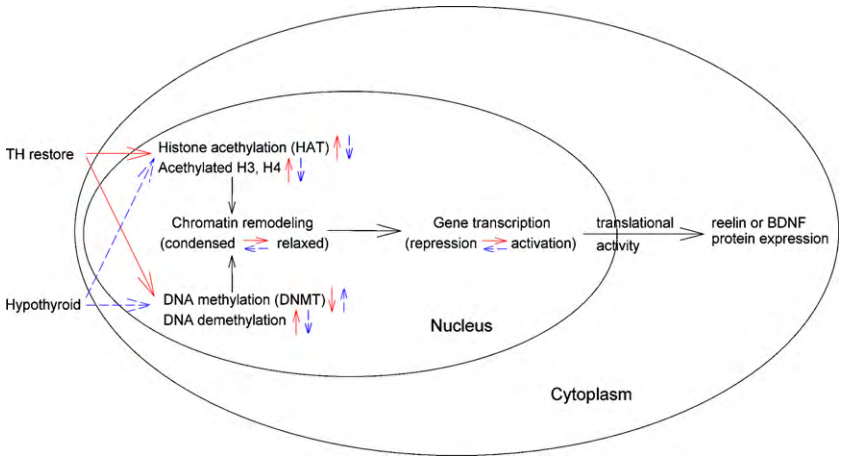

Fig. 6. Schematic representation of proposed mechanisms for the perinatal hypothyroidism on the regulation of *reelin* and *BDNF* exon II expression. Thyroid hormone (TH) treatment (solid arrow) and hypothyroidism (short dash arrow) may modulate the activities of HAT and the levels of acetylated H3, acetylated H4 and/or may modify DNA by influencing methylation states via demethylases or DNA methyltransferases (DNMT). These events lead to the chromatin remodeling, and then alteration in *reelin* and *BDNF* gene transcription.

hormone-mediated transcription. Our study further demonstrated that histone acetylation patterns, global acetylated H3 and global acetylated H4, were reduced in the hippocampus at the developmental stage in the hypothyroid animals. Even though these findings were consistent with Karsanov's study [51], however, these results have some differences from the previous studies. For example, in Lakshmy's study, PTU treatment only resulted in significant reduction in acetylated H3 at PND 21, and no changes in acetylated H4 [22]. In Tikoo's study, the levels of histone acetylation in liver tissue were not influenced by hypothyroidism [23]. These discrepancies may arise from differences in animal strain, tissues type, sampling time, the animal model of hypothyroidism used in the study, or other factors.

Histone acetylation regulates gene transcription at two levels: global histone acetylation and promoter-specific histone acetylation. In the present study, acetylated H3 and acetylated H4 at *reelin* promoter and at *BDNF* promoter for exon II were also reduced in the hypothyroid hippocampus at the developmental stage. Histone acetylation near enhancer and minimal promoter regions has been shown to play key roles in transcriptional activation and promoter-specific acetylation is a critical mechanism for control of specific gene activity [52]. Thus, reduced acetylation of H3 and H4 at *reelin* promoter and at *BDNF* promoter for exon II could account for the suppression of these genes mRNA expression in the hypothyroid hippocampus.

Both DNA methylation and histone acetylation are strongly implicated in regulating gene expression. Based on our results, a mechanism of perinatal hypothyroidism on the regulation of *reelin* and *BDNF* exon II expression in rat hippocampus was thus proposed (Fig. 6). It is more likely that these two perinatal hypothyroidism-induced epigenetic modulations of DNA methylation and histone acetylation and their cross-talks involve in the process of chromatin reorganization or remodeling, and thus influence the *reelin* and *BDNF* expression. The sequence and the timing of these two epigenetic mechanisms might be tissue-, animal age-, and gene promoter-, specific.

Previous studies have identified that numerous thyroid hormone-responsive genes are sensitive to perinatal hypothyroidism only during critical windows of brain development and expressions of these genes can reach the normal ranges in the adults [1,53–55]. Our results also revealed that suppression of *reelin* and *BDNF* exon II mRNA and protein expressions in rat hippocampus induced by perinatal hypothyroidism was only found at the early developmental stage, consisting with the previous studies [10,56–59]. Our findings further indicate that alterations in gene expressions at the early life stage may involve the two epigenetic mechanisms of DNA methylation and histone acetylation. Even though our results supported the notion of epigenetic modification of chromatin playing an important role in regulating gene expression during neuronal development [60–62], however, the reason why the epigenetic mechanism of DNA methylation and histone acetylation may not critical for the hypothyroidism-induced alterations in *reelin* and *BDNF* exon II expression at the later developmental stage or in the adults was not clear. The activities of DNMTs [63] and HATs [64,65] are attenuating with maturation and aging may be one of the reasons.

In summary, the present study demonstrated that DNA methylation and histone acetylation may play a role in the perinatal hypothyroidism-induced regulation of *reelin* and *BDNF* exon II expression in the developmental rat hippocampus. Collected with previous studies [22,47], epigenetic modifications of chromatin might be one of mechanisms underlying the adverse neurological effects observed in the perinatal hypothyroid animals.

Acknowledgements

This work was supported by grants to B.M. Li from the Ministry of Science and Technology of China (2006CB500807), the Ministry of Education of China (Program for Changjiang Scholars and Innovative Research Team in University), and the National Natural Science Foundation of China (30225023, 30430240, and 30611120530), and supported by the National Natural Science Foundation of China (30670673 and 30870823) and Innovation Program of Shanghai Municipal Education Commission to L. Sui.

References

[1] Bernal J, Guadaño-Ferraz A, Morte B. Perspectives in the study of thyroid hormone action on brain development and function. Thyroid 2003;13:1005–12.
[2] Tremont G, Stern RA, Westervelt HJ, Bishop CL, Davis JD. Neurobehavioral functioning in thyroid disorders. Med Health R I 2003;86:318–22.
[3] Leonard JL. Non-genomic actions of thyroid hormone in brain development. Steroids 2008;73:1008–12.
[4] Zhang J, Lazar MA. The mechanism of action of thyroid hormones. Annu Rev Physiol 2000;62:439–66.
[5] Koenig RJ. Thyroid hormone receptor coactivators and corepressors. Thyroid 1998;8:703–13.
[6] Oppenheimer JH, Schwartz HL. Molecular basis of thyroid hormone-dependent brain development. Endocr Rev 1997;18:462–75.
[7] Bernal J, Guadaño-Ferraz A. Analysis of thyroid hormone-dependent genes in the brain by in situ hybridization. Methods Mol Biol 2002;202:71–90.

[8] Herz J, Chen Y. Reelin lipoprotein receptors and synaptic plasticity. Nat Rev Neurosci 2006;7:850–9.
[9] Lu B, Figurov A. Role of neurotrophins in synapse development and plasticity. Rev Neurosci 1997;8:1–12.
[10] Manzano J, Morte B, Scanlan TS, Bernal J. Differential effects of triiodothyronine and the thyroid hormone receptor beta-specific agonist GC-1 on thyroid hormone target genes in the brain. Endocrinology 2003;144:5480–7.
[11] Alvarez-Dolado M, Iglesias T, Rodríguez-Peña A, Bernal J, Muñoz A. Expression of neurotrophins and the trk family of neurotrophin receptors in normal and hypothyroid rat brain. Brain Res Mol 1994;27:249–57.
[12] Camboni D, Roskoden T, Schwegler H. Effect of early thyroxine treatment on brain-derived neurotrophic factor mRNA expression and protein amount in the rat medial septum/diagonal band of Broca. Neurosci Lett 2003;350:141–4.
[13] Koibuchi N, Fukuda H, Chin WW. Promoter-specific regulation of the brain-derived neurotropic factor gene by thyroid hormone in the developing rat cerebellum. Endocrinology 1999;140:3955–61.
[14] Koibuchi N, Yamaoka S, Chin WW. Effect of altered thyroid status on neurotrophin gene expression during postnatal development of the mouse cerebellum. Thyroid 2001;11:205–10.
[15] Vaidya VA, Castro ME, Pei Q, Sprakes ME, Grahame-Smith DG. Influence of thyroid hormone on 5-HT(1A) and 5-HT(2A) receptor-mediated regulation of hippocampal BDNF mRNA expression. Neuropharmacology 2001;40:48–56.
[16] Lüesse HG, Roskoden T, Linke R, Otten U, Heese K, Schwegler H. Modulation of mRNA expression of the neurotrophins of the nerve growth factor family and their receptors in the septum and hippocampus of rats after transient postnatal thyroxine treatment. I. Expression of nerve growth factor, brain-derived neurotrophic factor, neurotrophin-3, and neurotrophin 4 mRNA. Exp Brain Res 1998;119:1–8.
[17] Egger G, Liang G, Aparicio A, Jones PA. Epigenetics in human disease and prospects for epigenetic therapy. Nature 2004;429:457–63.
[18] Jenuwein T, Allis CD. Translating the histone code. Science 2001;293:1074–80.
[19] Wong NC, Schwartz HL, Strait K, Oppenheimer JH. Thyroid hormone-, carbohydrate, and age-dependent regulation of a methylation site in the hepatic S14 gene. Mol Endocrinol 1989;3:645–50.
[20] Jump DB, Wong NC, Oppenheimer JH. Chromatin structure and methylation state of a thyroid hormone-responsive gene in rat liver. J Biol Chem 1987;262:778–84.
[21] Danzi S, Dubon P, Klein I. Effect of serum triiodothyronine on regulation of cardiac gene expression: role of histone acetylation. Am J Physiol Heart Circ Physiol 2005;289:H1506–11.
[22] Lakshmy R, Khurana ML, Das BC, Shah P, Ammini AC. Effect of PTU treatment on histone acetylation pattern in the developing rat brain. Endocr Res 1999;25:77–85.
[23] Tikoo K, Ali Z. Structure of active chromatin: covalent modifications of histones in active and inactive genes of control and hypothyroid rat liver. Biochem J 1997;322:281–7.
[24] Koibuchi N, Matsuzaki S, Ichimura K, Ohtake H, Yamaoka S. Effect of perinatal hypothyroidism on expression of cytochrome c oxidase subunit I gene, which is cloned by differential plaque screening from the cerebellum of newborn rat. J Neuroendocrinol 1995;7:847–53.
[25] Koibuchi N, Matsuzaki S, Ichimura K, Ohtake H, Yamaoka S. Ontogenic changes in the expression of cytochrome c oxidase subunit I gene in the cerebellar cortex of the perinatal hypothyroid rat. Endocrinology 1996;137:5096–108.
[26] Martinez de Arrieta C, Koibuchi N, Chin WW. Coactivator and corepressor gene expression in rat cerebellum during postnatal development and the effect of altered thyroid status. Endocrinology 2000;14:1693–8.
[27] Levenson JM, Roth TL, Lubin FD, Miller CA, Huang IC, Desai P, et al. Evidence that DNA (cytosine-5) methyltransferase regulates synaptic plasticity in the hippocampus. J Biol Chem 2006;281:15763–73.
[28] Nelson ED, Kavalali ET, Monteggia LM. Activity-dependent suppression of miniature neurotransmission through the regulation of DNA methylation. J Neurosci 2008;28:395–406.
[29] Miller CA, Sweatt JD. Covalent modification of DNA regulates memory formation. Neuron 2007;53:857–69.
[30] Aid T, Kazantseva A, Piirsoo M, Palm K, Timmusk T. Mouse and rat BDNF gene structure and expression revisited. J Neurosci Res 2007;85:525–35.
[31] Chakrabarti SK, James JC, Mirmira RG. Quantitative assessment of gene targeting in vitro and in vivo by the pancreatic transcription factor, Pdx1. Importance of chromatin structure in directing promoter binding. J Biol Chem 2002;277:13286–93.
[32] Sui LWWR, Li BM. Administration of thyroid hormone increased reelin and brain-derived neurotrophic factor expression in rat hippocampus in vivo. Brain Res 2010;1313:9–24.
[33] Sui L, Wang J, Li BM. Administration of triiodo-L-thyronine into dorsal hippocampus alters phosphorylation of Akt, mammalian target of rapamycin, p70S6 kinase and 4E-BP1 in rats. Neurochem Res 2008;33:1065–76.
[34] Sui L, Wang J, Li BM. Role of the phosphoinositide 3-kinase-Akt-mammalian target of the rapamycin signaling pathway in long-term potentiation and trace fear conditioning memory in rat medial prefrontal cortex. Learn Mem 2008;15:762–76.
[35] O'Connor JC, Frame SR, Davis LG, Cook JC. Detection of thyroid toxicants in a tier I screening battery and alterations in thyroid endpoints over 28 days of exposure. Toxicol Sci 1999;51:54–70.
[36] Wolffe AP, Matzke MA. Epigenetics: regulation through repression. Science 1999;286:481–6.
[37] Klose RJ, Bird AP. Genomic DNA methylation: the mark and its mediators. Trends Biochem Sci 2006;31:89–97.
[38] Bird AP, Wolffe AP. Methylation-induced repression—belts, braces, and chromatin. Cell 1999;99:451–4.
[39] Bird A. DNA methylation patterns and epigenetic memory. Genes Dev 2002;16:6–21.
[40] Reik W, Kelsey G, Walter J. Dissecting de novo methylation. Nat Genet 1999;23:380–2.
[41] Jaenisch R, Bird A. Epigenetic regulation of gene expression: how the genome integrates intrinsic and environmental signals. Nat Genet 2003;33:245–54.
[42] Li E, Bestor TH, Jaenisch R. Targeted mutation of the DNA methyltransferase gene results in embryonic lethality. Cell 1992;69:915–26.
[43] Rakyan VK, Preis J, Morgan HD, Whitelaw E. The marks, mechanisms and memory of epigenetic states in mammals. Biochem J 2001;356:1–10.
[44] Davis FJ, Pillai JB, Gupta M, Gupta MP. Concurrent opposite effects of trichostatin A, an inhibitor of histone deacetylases, on expression of alpha-MHC and cardiac tubulins: implication for gain in cardiac muscle contractility. Am J Physiol Heart Circ Physiol 2005;288:H1477–90.
[45] McKinsey TA, Olson EN. Cardiac histone acetylation—therapeutic opportunities abound. Trends Genet 2004;20:206–13.
[46] Xu L, Glass CK, Rosenfeld MG. Coactivator and corepressor complexes in nuclear receptor function. Curr Opin Genet Dev 1999;9:140–7.
[47] Dong H, Wade M, Williams A, Lee A, Douglas GR, Yauk C. Molecular insight into the effects of hypothyroidism on the developing cerebellum. Biochem Biophys Res Commun 2005;330:1182–93.
[48] Li Q, Sachs L, Shi YB, Wolffe AP. Modification of chromatin structure by the thyroid hormone receptor. Trends Endocrinol Metab 1999;10:157–64.
[49] McKenna NJ, Xu J, Nawaz Z, Tsai SY, Tsai MJ, O'Malley BW. Nuclear receptor coactivators: multiple enzymes, multiple complexes, multiple functions. J Steroid Biochem Mol Biol 1999;69:3–12.
[50] Sánchez-Pacheco A, Aranda A. Binding of the thyroid hormone receptor to a negative element in the basal growth hormone promoter is associated with histone acetylation. J Biol Chem 2003;278:39383–91.
[51] Karsanov NV, Dzhagarov DE. RNA synthesis and modifications of heart nuclear proteins during thyroid hormone deficiency. Mol Biol (Mosk) 1979;13:38–46.
[52] Gottesfeld JM, Forbes DJ. Mitotic repression of the transcriptional machinery. Trends Biochem Sci 1997;22:197–202.
[53] Koibuchi N, Jingu H, Iwasaki T, Chin WW. Current perspectives on the role of thyroid hormone in growth and development of cerebellum. Cerebellum 2003;2:279–89.
[54] Bernal J. Action of thyroid hormone in brain. J Endocrinol Invest 2002;25:268–88.
[55] Thompson CC, Potter GB. Thyroid hormone action in neural development. Cereb Cortex 2000;10:939–45.
[56] Neveu I, Arenas E. Neurotrophins promote the survival and development of neurons in the cerebellum of hypothyroid rats in vivo. J Cell Biol 1996;133:631–46.
[57] Kobayashi K, Tsuji R, Yoshioka T, Mino T, Seki T. Perinatal exposure to PTU delays switching from NR2B to NR2A subunits of the NMDA receptor in the rat cerebellum. Neurotoxicology 2006;27:284–90.
[58] Sinha RA, Pathak A, Kumar A, Tiwari M, Shrivastava A, Godbole MM. Enhanced neuronal loss under perinatal hypothyroidism involves impaired neurotrophic signaling and increased proteolysis of p75(NTR). Mol Cell Neurosci 2009;40:354–64.
[59] Alvarez-Dolado M, Ruiz M, Del Río JA, Alcántara S, Burgaya F, Sheldon M, et al. Thyroid hormone regulates reelin and dab1 expression during brain development. J Neurosci 1999;19:6979–93.
[60] Kiefer JC. Epigenetics in development. Dev Dyn 2007;236:1144–56.
[61] Feng J, Fouse S, Fan G. Epigenetic regulation of neural gene expression and neuronal function. Pediatr Res 2007;61:58R–63R.
[62] Keverne EB, Curley JP. Epigenetics, brain evolution and behaviour. Front Neuroendocrinol 2008;29:398–412.
[63] Singh K, Prasad S. Age- and sex-related analysis of methylation of 5′-upstream sequences of Fmr-1 gene in mouse brain and modulation by sex steroid hormones. Biogerontology 2008;9:455–65.
[64] Piña B, Martínez P, Suau P. Differential acetylation of core histones in rat cerebral cortex neurons during development and aging. Eur J Biochem 1988;174:311–5.
[65] Li Q, Xiao H, Isobe K. Histone acetyltransferase activities of cAMP-regulated enhancer-binding protein and p300 in tissues of fetal, young, and old mice. J Gerontol A: Biol Sci Med Sci 2002;57:B93–8.